Journal of Alloys and Compounds 756 (2018) 126–133

Contents lists available at ScienceDirect

Journal of Alloys and Compounds

journal homepage: http://www.elsevier.com/locate/jalcom

Review

Photoluminescence, thermo- and optically stimulated luminescence properties of Eu^{3+} doped $Sr_2P_2O_7$ synthesized by the solvent evaporation method

J. Roman-Lopez [a, *], M. Valverde [b], M. García-Hipólito [c], I.B. Lozano [d], J.A.I. Diaz-Góngora [d]

[a] CONACYT-Instituto de Ciencias Nucleares, Universidad Nacional Autónoma de México, A.P.70-543, 04510, Ciudad de México, México
[b] Instituto de Ciencias Nucleares, Universidad Nacional Autónoma de México, A.P. 70-543, 04510, Ciudad de México, México
[c] Instituto de Investigaciones en Materiales, Universidad Nacional Autónoma de México, A.P. 70-543, 04510, Ciudad de México, México
[d] Instituto Politécnico Nacional, Centro de Investigación en Ciencia Aplicada y Tecnología Avanzada, Unidad Legaria, 11500, Ciudad de México, México

ARTICLE INFO

Article history:
Received 31 January 2018
Received in revised form
27 April 2018
Accepted 28 April 2018
Available online 30 April 2018

Keywords:
Solvent evaporation method
Strontium pyrophosphate
Eu^{3+} ions
Luminescence properties

ABSTRACT

In this research, undoped and Eu^{3+} (0.5, 1, 3, 5, 8 and 10 mol%) doped strontium pyrophosphate ($Sr_2P_2O_7$) powders were synthesized by the solvent evaporation method and their luminescence properties were studied by photoluminescence (PL), thermoluminescence (TL) and, for the first time, optically stimulated luminescence in continuous wave modality (CW-OSL). The $Sr_2P_2O_7$:Eu^{3+} material was structural and morphological characterized using X-ray diffraction (XRD) and Scanning Electron Microscopy (SEM). The PL excitation and emission spectra exhibited transitions related to Eu^{3+} ions into the $Sr_2P_2O_7$ host lattice. In the excitation spectrum an intense broad charge transfer band around 267 nm was observed in all doped samples. A chemical reduction process of the Eu^{3+} ions incorporated in the $Sr_2P_2O_7$ host is carried out when the samples are exposed to ^{90}Sr beta particles and it is a crucial factor in the TL and CW-OSL responses. The TL response of the Eu^{3+} doped $Sr_2P_2O_7$ samples, displays light emissions associated with the presence of Eu^{3+} and Eu^{2+} ions. The undoped $Sr_2P_2O_7$ showed TL maxima at 95, 150 and 230 °C and CW-OSL fast decay when the samples are stimulated with infrared light. All $Sr_2P_2O_7$ and $Sr_2P_2O_7$:Eu^{3+} (0.5 and 1 mol%) samples showed TL and CW-OSL linear response in the range of 0.5–25 Gy and acceptable repeatability with a variation coefficient lower than 5%. Using CW-OSL and TL dose-response the minimum detectable dose was estimated as 2 mGy (TL-0.5 mol%), 3 mGy (TL-1 mol%), 14 mGy (TL-undoped) and 2 mGy (CW-OSL-undoped).

Contents

* Corresponding author.
E-mail address: jesus.roman@nucleares.unam.mx (J. Roman-Lopez).

https://doi.org/10.1016/j.jallcom.2018.04.314
0925-8388/

1. Introduction

The luminescent materials (phosphors) are studied for technological applications due to their ability to emit visible light when are irradiated with different types of radiation, for example, gamma radiation, β particles, X-ray and ultraviolet (UV) light. Pure and doped (Ca, Sr and Ba) pyrophosphates are used as host lattices for phosphors and recently some studies showed that the incorporation of lanthanide ions into the pyrophosphate structure provide chemical stability and interesting properties applicable to display devices, light emitting diodes, flat panel displays and dosimetry materials [1,2]. In this context, the strontium pyrophosphate ($Sr_2P_2O_7$) has shown good structure characteristics for the incorporation of luminescent ions. This material exhibits two polymorphs: low temperature β-$Sr_2P_2O_7$ and elevated temperature α-$Sr_2P_2O_7$, the phase transition occurs at about 760–780 °C. There are two types of sites for Sr^{2+} (Sr_1 and Sr_2) ions in the $Sr_2P_2O_7$ unit cell, both Sr^{2+} sites are coordinated by nine oxygen ions with average bond lengths of 2.721 Å and 2.679 Å, respectively [3]. α-$Sr_2P_2O_7$ contains four molecules per unit cell and has cell parameters of: a = 8.917 Å, b = 13.173 Å, c = 5.400 Å [4]. Since the development of $Sr_2P_2O_7$:Eu^{2+} materials diverse investigations are oriented to study the luminescence properties of $Sr_2P_2O_7$ doped with rare earth ions and transition metal ions. The $Sr_2P_2O_7$:Eu^{2+} phosphor is used in fluorescent lamps due to its high quantum efficiency (~90%) [5]. In another investigation, the Y^{3+} co-doped $Sr_2P_2O_7$:Eu^{2+} showed a long-lasting blue phosphorescence up to 8 h after turned off the UV light excitation at 254 nm. This lasting blue emission could be related to the energy transfer process from traps created by the incorporation of Y^{3+} ions [6]. Peng and Wondraczek [7] discussed the energy transfer process and red emission emitted by the $Sr_2P_2O_7$:Bi^{2+} compound. This transfer process occurred between two Bi^{2+} ions incorporated in both Sr_1 and Sr_2 lattice sites. The Bi^{2+} ions located on Sr_1 site emit at 667 nm whereas the Bi^{2+} ions on Sr_2 emits at 700 nm. The luminescence properties of $Sr_2P_2O_7$:Eu^{3+},M (M = Li^+, Na^+, K^+) were studied by Fan et al. [8]. It is found that the $Sr_2P_2O_7$:Eu^{3+},Na^+ shows the best emission intensity and enhancement of the $^5D_0 \rightarrow {}^7F_2$ transition at 610 nm due to the charge compensator effect and the improved crystallinity. On the other hand, thermally stimulated luminescence (thermoluminescence, TL) emissions were studied on $Sr_2P_2O_7$:Eu^{3+}, $Sr_2P_2O_7$:Ce^{3+} and $Sr_2P_2O_7$:Tb^{3+} phosphors. A TL glow curve composed by two peaks around 192 and 292 °C was observed in ^{60}Co gamma irradiated $Sr_2P_2O_7$:Eu^{3+} samples [9]. Similar temperature peak at 192 °C was shown by $Sr_2P_2O_7$ samples doped with Ce^{3+} ions after exposed to X-ray irradiation [10]. Furthermore, two TL glow peaks at 147 and 252 °C were found in Tb^{3+} doped $Sr_2P_2O_7$ phosphors irradiated using ^{90}Sr β-source [11]. In this work, the luminescence properties of $Sr_2P_2O_7$ and $Sr_2P_2O_7$:Eu^{3+} powders synthesized by solvent evaporation method were studied using photoluminescence, thermoluminescence and, for the first time, optically stimulated luminescence. In addition, the structural and morphological characteristics of $Sr_2P_2O_7$:Eu^{3+} powders were analyzed by XRD and SEM, respectively.

2. Materials and methods

2.1. Synthesis of $Sr_2P_2O_7$ and $Sr_2P_2O_7$:Eu^{3+} powders

The strontium pyrophosphate ($Sr_2P_2O_7$) undoped and doped with Eu^{3+} ions were synthesized through the simple solvent evaporation method. $SrCl_2$ (analytical grade), $(NH_4)_2HPO_4$ (99% purity) and $EuCl_3$ (0.5, 1, 3, 5, 8 and 10 mol%) (99.9% purity), mixed with deionized water in stoichiometric quantities, were used as precursor reagents for obtaining the $Sr_2P_2O_7$ and $Sr_2P_2O_7$:Eu^{3+} samples. Then, the solvent was evaporated at 250 °C by a time of 45 min. Finally, the obtained $Sr_2P_2O_7$ and $Sr_2P_2O_7$:Eu^{3+} powders were placed into an alumina crucible and annealed at 900 °C for 18 h.

2.2. Structural (XRD) and morphological (SEM) analyses

Structural characterization of the $Sr_2P_2O_7$:Eu^{3+} (1 mol%) powders were carried out by X-ray diffraction in a D-8 advance Bruker diffractometer using Cu-Kα radiation (λ = 1.5406 Å). The XRD patterns were measured from 10° up to 70° (2θ in steps of 0.020° and 1.5 s per step). $Sr_2P_2O_7$:Eu^{3+} powders were ground in an agate mortar and sifted up to a particle size <17 μm was obtained. The sifted powders were collocated on copper grids and covered with carbon for SEM analysis in a Field Emission Scanning Electron Microscope JEOL model JSM-7800 F. The SEM images of the $Sr_2P_2O_7$:Eu^{3+} sample was scanned by an electron beam at 15 kV.

2.3. Luminescence properties of PL, TL and CW-OSL

Luminescence properties of $Sr_2P_2O_7$ and $Sr_2P_2O_7$:Eu^{3+} samples were studied by photoluminescence excitation (PLE) and emission (PL) spectra, thermoluminescence (TL) and optically stimulated luminescence (CW-OSL). PLE and PL spectra were measured at room temperature (RT) in a Horiba Jobin-Yvon Fluoro-Max-P fluorescence spectrophotometer. Aliquots of 0.8 mg (<149 μm) were weighted and mounted into aluminum disks using silicon oil. All samples were irradiated using a ^{90}Sr β-source with dose rate of 0.12 Gy/s and analyzed by TL and CW-OSL in an automatic TL/OSL Lexsyg Research equipment. The TL measurements were acquired from RT (~25 °C) up to 300 °C with a linear heating rate of 2 °C/s and detection windows centered at 414 and 575 nm. CW-OSL readings of the samples were performed for 60 s with infrared light stimulation peaked at 850 nm and powered by 10 mW/cm^2. The CW-OSL emissions of the samples were observed through a set of optical filters (Schott BG-39 and Semrock FF01-414/46) to obtain a detection window peaked at 414 nm and FWHM bandwidth of 50 nm. One aliquot was used for each TL and CW-OSL measurement.

3. Results and discussion

3.1. Structural characterization

The XRD pattern of the $Sr_2P_2O_7$ doped with Eu^{3+} (1 mol%) is shown in Fig. 1a. The XRD pattern of the sample shows the pure phase of $Sr_2P_2O_7$ without the formation of other undesirable phases and matched well with the standard JCPDS file 024-1011 (red vertical lines in Fig. 1a). The structural characteristic of the powders corresponds to alpha phase (α-$Sr_2P_2O_7$) with centrosymmetric spaced group *Pnma (62)*, orthorhombic crystalline system and cell parameters of a = 8.917 Å, b = 13.169 Å and c = 5.400 Å. These XRD data agree with those reported in the literature [8].

3.2. Surface morphology of $Sr_2P_2O_7$:Eu^{3+}

The $Sr_2P_2O_7$:Eu^{3+} (1 mol%) powders show a surface morphology constituted by polycrystalline irregular particles with sizes between 1 and 4 μm distributed homogeneously over the whole sample and the formation of some agglomerates is also observed, the above is shown in Fig. 1b. In the inset of Fig. 1b can be appreciated a detail the size and shape of the particles. The crystalline phase, size and morphology of the particles are important characteristics of a luminescent material because they affect, to some extent, the position and intensity of the PL emissions. In particular, luminescent materials with larger grain size such as Ln^{3+} doped

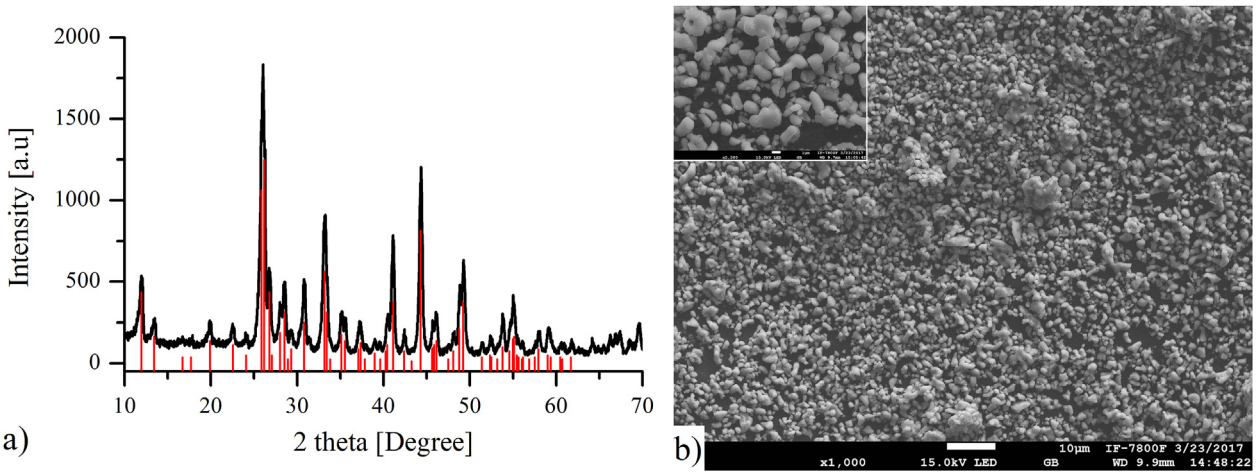

Fig. 1. a) XRD pattern (red lines correspond to 024-1011 file) and b) SEM image of $Sr_2P_2O_7$ doped with 1 mol% Eu^{3+}. Inset shows in some detail the shape and size of the $Sr_2P_2O_7$:Eu^{3+} particles. (For interpretation of the references to colour in this figure legend, the reader is referred to the Web version of this article.)

fluoride (β-$NaGdF_4$:Eu^{3+}) presents higher emission efficiency [12]. In this sense, the synthesized $Sr_2P_2O_7$:Eu^{3+} (1 mol%) powders present a well-defined orthorhombic crystalline phase (according to Fig. 1), proper particle size and homogeneous morphology for its use as luminescent material. It is well known that the method of synthesis affects strongly the morphology (shape and size) of the powders. Several authors obtained $Sr_2P_2O_7$ powders using methods such as chemical precipitation [9], combustion synthesis [2,10,11] and high temperature solid state reaction [6–8]. In these investigations they do not reported the superficial morphology of the synthesized samples and they do not correlated the luminescence properties of the samples with the shape and size of the particles. Wang et al. [13] reported the formation of flowerlike microspheres in green strong emitted $Sr_{1.92}P_2O_7$:0.06Ce^{3+},0.02 Tb^{3+} powders synthesized by microwave-assisted co-precipitation reaction. Similar morphology was observed in $Sr_2P_2O_7$:Ce^{3+},Mn^{2+} phosphors synthesized by co-precipitation method. It was concluded that the observed spherical morphology improves the luminescence properties [14]. The solvent evaporation method has been extensively used to synthesize photoluminescence [15,16] and thermoluminescence [17,18] materials due to it can be applied at relatively low temperatures and provide homogeneity and particle size controllability [19]. For these reasons, we employed the solvent evaporation method to synthesize the $Sr_2P_2O_7$ and $Sr_2P_2O_7$:Eu^{3+} powders.

3.3. Photoluminescence analysis

Photoluminescence emissions were studied using the excitation (PLE) and emission (PL) spectra of the $Sr_2P_2O_7$:Eu^{3+} samples (0.5, 1, 3, 5, 8 and 10 mol%) measured at RT (~25 °C). The PLE spectrum, monitored at 612 nm associated with the $^5D_0 \rightarrow {}^7F_2$ characteristic emission of Eu^{3+} ions, exhibits an intense broad excitation band ranging from 230 nm to 315 nm (centered at 267 nm) and five narrow lines at 319 ($^7F_0 \rightarrow {}^5H_5$), 362 ($^7F_0 \rightarrow {}^5D_4$), 377 ($^7F_0 \rightarrow {}^5G_3$), 382 ($^7F_0 \rightarrow {}^5L_7$) and 394 nm ($^7F_0 \rightarrow {}^5L_6$) (Fig. 2a, left). A charge transfer (CT) from O^{2-} to Eu^{3+} atoms is responsible of the broad excitation band, the Eu^{3+} ions present a partially-filled $4f^6$ configuration that is less stable than the half-filled $4f^7$ configuration [20,21]. As seen in Fig. 2a, right, PL spectrum ($\lambda_{ex} = 267$ nm) of $Sr_2P_2O_7$:Eu^{3+} shows six emissions peaks centered at 536, 555, 593, 612, 652 and 698 nm corresponding respectively to the $^5D_1 \rightarrow {}^7F_{1,2}$, $^5D_0 \rightarrow {}^7F_1$, $^5D_0 \rightarrow {}^7F_2$, $^5D_0 \rightarrow {}^7F_3$, and $^5D_0 \rightarrow {}^7F_4$ Eu^{3+} transitions. Such behavior has been observed regardless of the matrix (phosphates, or aluminates) and/or the luminescence process (PL [22] or CL [23]). The magnetic dipole transition $^5D_0 \rightarrow {}^7F_1$ (593 nm) is insensitive to the symmetry, whereas that the intense electric dipole transition $^5D_0 \rightarrow {}^7F_2$ (612 nm) is induced by the lack of inversion symmetry at the Eu^{3+} sites [22,24]. The local symmetry of the atoms around Eu^{3+} ions can be measure using the intensity ratio ($R = IF_2/IF_1$) between $^5D_0 \rightarrow {}^7F_2$ and $^5D_0 \rightarrow {}^7F_1$ transitions [25,26]. The intensity of both transitions (IF_2 and IF_1) was calculated using the area from 570 to 603 nm and 604–642 nm, respectively. The variation of the intensity ratio presented values of 2.11, 2.3, 1.56, 1.44, 1.65 and 1.68 for a Eu^{3+} content of 0.5, 1, 3, 5, 8 and 10 mol%, respectively. These values ($R > 1$) indicated that the Eu^{3+} ions are incorporated into the $Sr_2P_2O_7$ host lattice with a low symmetry, in the case of the sample doped with 1 mol% Eu^{3+} it exhibits more symmetry than those with other Eu^{3+} content. Fig. 2b depicts the influence of Eu^{3+} content in the emission intensity of the PL spectrum ($\lambda_{ex} = 267$ nm) and in the ratio R (inset of Fig. 2b). It is well known that the intensity of the PL emissions increases as doping content up to a quenching concentration where the PL intensity decreases. According to the inset of Fig. 2b (red circles) the quenching concentration was found at around 8 mol% Eu^{3+} and a light recovery of the integrated PL intensity was observed in 10 mol % of Eu^{3+} content. The best integrated PL intensity is shown by the $Sr_2P_2O_7$:Eu^{3+} sample doped with 5 mol%. The concentration quenching could be influenced by the amount of Sr vacancies (V''_{Sr}) and oxygen interstitials (O''_i). Han et al. [27] proposed that the luminescence intensity of the $Sr_2P_2O_7$:Dy samples is affected by the presence of V''_{Sr} and O''_i defects which were generated by the addition of the Dy^{3+} ions. In this study, probably the incorporation of Eu^{3+} into the $Sr_2P_2O_7$ lattice produce these defects that cause a decrease of the luminescence intensity. The V''_{Sr} defect is observed when two Eu^{3+} ions substitute three Sr^{2+} and the O''_i defect appears in the crystal lattice whether two Sr^{2+} atoms are substituted by two Eu^{3+} ions. The luminescence intensity of the Eu^{3+} ions is reduced by energy transfer to V''_{Sr} vacancy and energy migration through O''_i interstitials.

3.4. TL and CW-OSL properties

According to the PL spectra and the available optical filters, the $Sr_2P_2O_7$:Eu^{3+} samples were analyzed by TL using a set of filters (Schott BG 39 and Semrock HC 575/25), centered at 575 nm with a bandwidth of 25 nm, for observing the $^5D_0 \rightarrow {}^7F_2$ (593 nm)

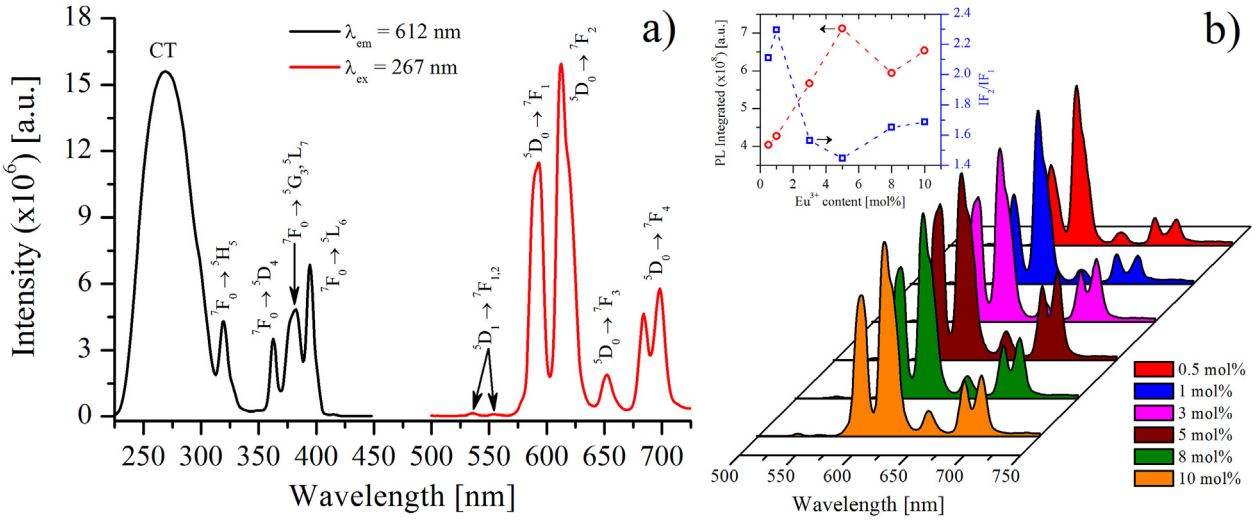

Fig. 2. a) PLE and PL spectra of $Sr_2P_2O_7$:Eu^{3+} (5 mol%) measured at room temperature using a $\lambda_{em} = 612$ nm and $\lambda_{ex} = 267$ nm, respectively, and b) PL spectra of $Sr_2P_2O_7$:Eu^{3+} doped with 0.5, 1, 3, 5, 8 and 10 mol% (inset displays the integrated PL intensity and the intensity ratio (R) as function of Eu^{3+} content).

emission of Eu^{3+}. The TL response of the green-yellow region (550–600 nm) exhibits glow maxima at 75, 162 and 230 °C for the samples doped with 0.5, 1 and 3 mol% Eu^{3+}, the 5, 8 and 10 mol% Eu^{3+} doped samples display glow maxima at 75 and 162 °C, finally the undoped sample shows TL maxima at 90, 150 and 230 °C, as illustrated in Fig. 3a. Nevertheless, the TL glow curve of the samples in the green-yellow region shows a very low intensity. Therefore, the TL response of the samples was studied in another range of wavelength such as 385–450 nm according to reported by Upadeo et al. [28]. It was found that Eu^{3+} ions in the $Sr_2P_2O_7$ lattice change the valence state to Eu^{2+} due to the interaction of the sample with the ionizing radiation. As consequence, the TL emissions of the samples were studied in the UV-blue region using a detection window centered at 414 nm and bandwidth of 46 nm. Fig. 3b displays the TL glow curves obtained with a test dose of 8 Gy. The undoped sample shows UV-blue TL maxima at 95, 150 and 230 °C which are similar to observed by Seyyidoğlu et al. [29] on pure $Sr_2P_2O_7$ samples. The $Sr_2P_2O_7$:Eu^{3+} samples displayed TL glow curves that exhibit maxima around of 79 and 160 °C (0.5 mol%), 85 and 161 °C (1 mol%), 82 and 162 °C (3 mol%), 57, 91 and 155 °C (5 mol%), 90 °C and 153 °C (8 mol%), and 86 °C and 148 °C (10 mol%) (Fig. 3b). The dispersion of the maxima in the TL glow curves could be related to the concentration of the Eu^{3+} ions incorporated in the $Sr_2P_2O_7$ crystal lattice, i.e. the quenching concentration affects the intensity and temperature of the glow maximum possibly to saturation of electron and hole traps, radiative and nonradiative recombination competition and/or different kinds of trapping centers [30]. Others compounds have shown TL maxima dispersion with the variation of Eu^{3+} concentration [31,32].

On the other hand, the enhancement of the TL intensity in $Sr_2P_2O_7$:Eu^{3+} samples measured at wavelength that correspond to UV-blue (385–450 nm) region confirms that a chemical reduction process is carried out in the Eu^{3+} ions ($Eu^{3+} \rightarrow Eu^{2+}$) when the samples are exposed to ^{90}Sr beta particles. Also, the observed TL response using the 575 nm set of optical filters (green-yellow region) implies that the concentration of Eu^{3+} ions is not all reduced

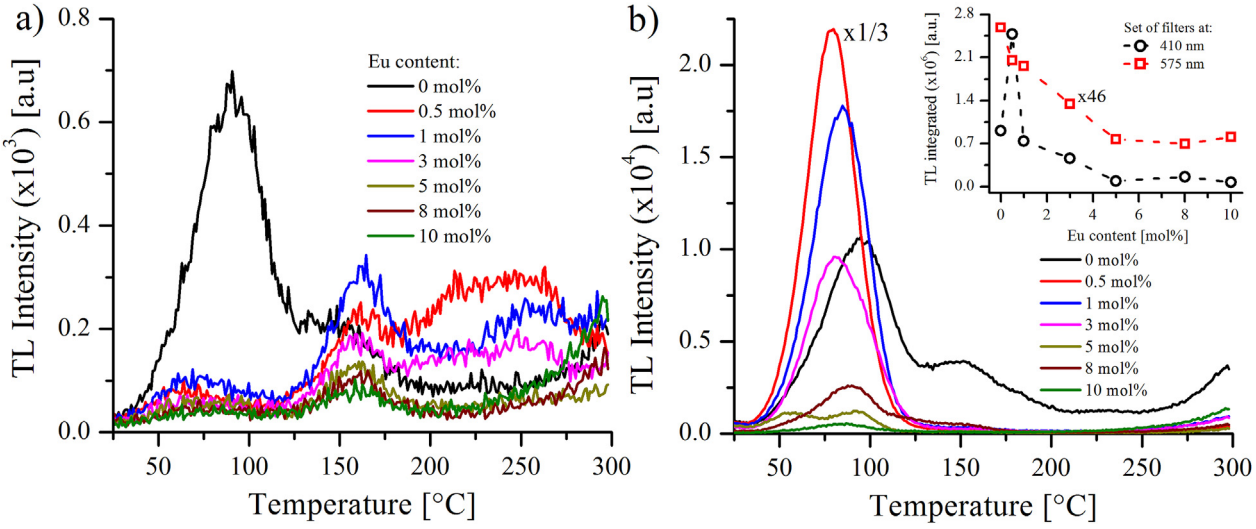

Fig. 3. TL glow curves measured on $Sr_2P_2O_7$ undoped and doped Eu^{3+} (0.5, 1, 3 5, 8 and 10 mol%) using a set of optical filters centered at a) 575 nm (green-yellow region) and b) 414 nm (UV-blue region). Inset shows the relation between the integrated TL response and Eu^{3+} content. The Eu^{3+} 0.5 mol% TL glow curve was multiplied by 1/3 and the 575 nm integrated TL response was multiplied by 46. (For interpretation of the references to colour in this figure legend, the reader is referred to the Web version of this article.)

to Eu^{2+} ions independent of the dose of radiation applied in the sample.

The low temperature maximum (95 and 90 °C) of the undoped sample in the UV-blue (370–460 nm) and green-yellow (550–600 nm) regions would be associated with structural defects in the lattice such as oxygen vacancies, substitution and interstitial atoms that create the localized charge losses [33] and has been also observed in some other synthetic phosphates [34]. These defects are created and increased during the growth and annealing of the sample, respectively. The maxima appearing in 150 and 230 °C (UV-blue and green-yellow regions) could be related to the recombination of PO_2^{2-} and O^{2-} radicals generated during the irradiation of the samples [9]. The TL maxima of the Eu^{3+} doped $Sr_2P_2O_7$ samples in the UV-blue and green-yellow regions should correspond respectively to Eu^{2+} and Eu^{3+} emissions excited by energy transfer from recombination centers associated to structural defects (low temperature maxima, 75–91 °C) and recombination of PO_2^{2-} and O^{2-} radicals (high temperature maxima, 155–162 °C and 230 °C).

Inset of Fig. 3b shows the integrated TL intensities for the Eu^{3+} contents studied with both 575 and 414 nm set of optical filters. For the integrated TL glow curve obtained in the green-yellow region the undoped sample shows an intense TL response than the others doped samples. In the case of the integrated TL glow curves obtained in the UV-blue region the sample doped with 0.5 mol% presented the more intense TL response than the other samples. For 3, 5, 8 and 10 mol% of Eu^{3+} the integrated TL response of the samples decreased drastically. At low doping concentration the substitutional incorporation of the Eu^{3+} impurities in Sr^{2+} sites are predominated whereas at high concentrations the interstitial incorporation of Eu^{3+} ions can be carried out. Previously, Patel et al. [35] studied the variation in TL intensity of ^{90}Sr (5–50 Gy) irradiated $Sr_2P_2O_7$:Eu^{3+} samples with concentrations from 0.1 mol% up to 5.0 mol%. They observed the higher TL intensity in samples with 0.1 mol% of Eu^{3+} ions. Hence, the $Sr_2P_2O_7$:Eu^{3+} samples doped with 3, 5, 8 and 10 mol% were not further analyzed due to its low TL integrated response.

For the first time the CW-OSL decay curves of $Sr_2P_2O_7$ and $Sr_2P_2O_7$:Eu^{3+} (0.5 and 1 mol%), irradiated at 8 Gy and stimulated with IR light (850 nm and 10 mW/cm^2) for 60 s, are analyzed. All the samples were measured using a detection window centered at 414 nm (UV-blue region) to study the Eu^{2+} blue emissions. Fig. 4a shows that the CW-OSL response of the $Sr_2P_2O_7$ sample is eleven and twenty-four times more intense than those doped with 0.5 and 1 mol% of Eu^{3+} ions. For times of 0.5 and 20 s of IR light stimulation, the CW-OSL intensity of the undoped and doped $Sr_2P_2O_7$ with 0.5 and 1 mol% of Eu^{3+} samples decayed 66% and 98%, 6% and 51%, 26% and 69%, respectively. The undoped $Sr_2P_2O_7$ sample showed a CW-OSL decay faster than the $Sr_2P_2O_7$:Eu^{3+} samples. In order to investigate the origin of the CW-OSL response the undoped and Eu^{3+} doped samples were firstly analyzed by TL (residual) after subsequent CW-OSL (Fig. 4a) and secondly preheated with a heating rate of 2 °C/s up to 120 °C to isolate the second group of components, cooled to room temperature, analyzed by CW-OSL and then the residual TL was measured (Fig. 4b). Inset of Fig. 4a displays the TL glow curve before and after subsequent CW-OSL response for undoped and 0.5 mol% Eu^{3+} doped samples. It was found that the TL intensity of the maxima at 95 °C and 150 °C in the undoped sample decrease after subsequent CW-OSL reading. The intensity of the maximum at 95 °C only decreases in the initial part which could be related to the presence of an overlapped maximum at low temperature than 95 °C. The TL intensity of the maximum at 90 °C of $Sr_2P_2O_7$:Eu^{3+} sample is little affected by the IR light of the CW-OSL measure, whereas the TL intensity of the maximum at 150 °C was not modified. In Fig. 4b is shown the CW-OSL response of the undoped and doped samples preheated at 120 °C. The CW-OSL intensity of the undoped sample decreases drastically (~71%) because the maximum at 95 °C were removed and only the traps associated with the maximum at 150 °C giving rise to the CW-OSL response. An important observation is the reappearing of the TL maximum at 95 °C (inset of Fig. 4b) which can be related with the phototransfer of charge carries from deep TL traps located at 150 °C to shallow traps under IR light stimulation. This confirms that the CW-OSL intensity of undoped samples is originated from the 95 and 150 °C maxima and the intensity of the maximum at 95 °C is improved by phototransfer. On the contrary, the TL intensity of the maximum at 150 °C of Eu^{3+} doped samples not change before and after subsequent CW-OSL readout, as well a maximum around at 90 °C is observed on the residual TL glow curve, in this sample the phototransfer of charge carries could be related to deeper traps

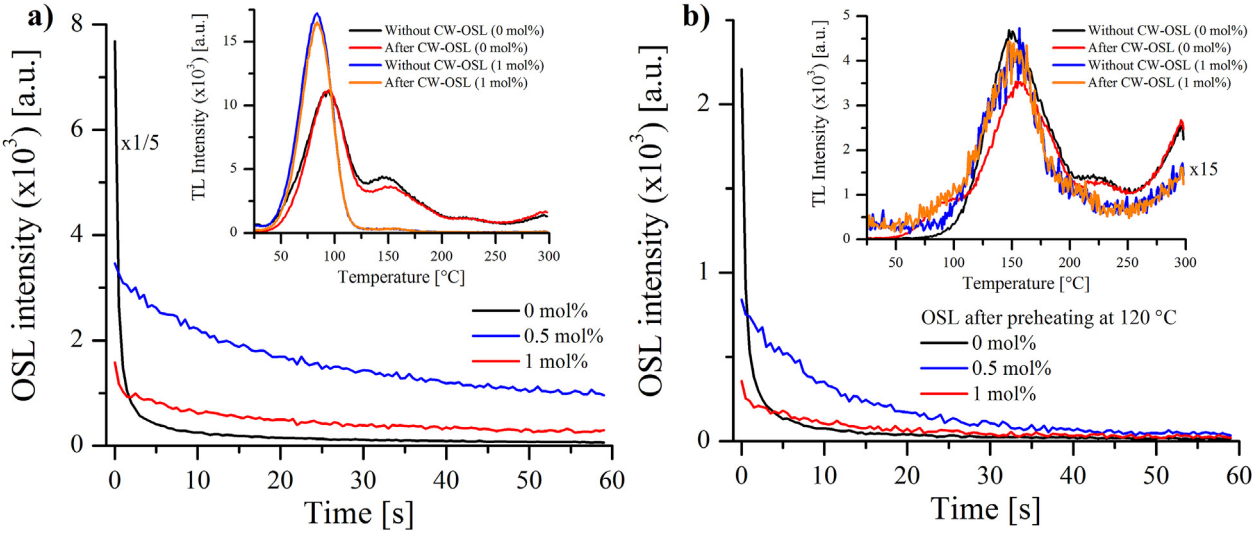

Fig. 4. CW-OSL decay curves of $Sr_2P_2O_7$ undoped and doped Eu^{3+} (0.5 and 1 mol%) samples recorded a) after irradiation and b) preheated at 120 °C with 2 °C/s heating rate. Insets of figures show the TL glow curves before and after IR light stimulation for 60 s. The undoped CW-OSL decay curve was multiplied by 1/5 and the preheated TL glow curves of Eu^{3+} (1 mol%) doped $Sr_2P_2O_7$ was multiplied by 15.

located over 300 °C, more studies are necessary to confirm this behavior.

The dose-response and repeatability experiments were performed on the undoped $Sr_2P_2O_7$ and doped with 0.5 and 1 mol% of Eu^{3+} samples with the purpose of study its possible application in the TL and CW-OSL fields. In dose-response test the samples were exposed to ^{90}Sr beta particles from 0.5 Gy to 25 Gy. As can be seen in Fig. 5, the TL and CW-OSL dose-response in the UV-blue region was fitted using a linear regression and the fit of each regression was monitored by the adjusted R-squared (r^2). In the TL dose-response each data was obtained from the integration of the whole TL curve and in the CW-OSL response the data was calculated from the difference between whole integrated data and the mean of the last ten points of the CW-OSL curve, i.e. the background of the CW-OSL intensity was subtracted of the integrated curves. The integrated TL and CW-OSL response of the samples showed a linear response in the whole dose range (0.5–25 Gy) with r^2 equal to 0.995 (TL-undoped), 0.997 (TL-0.5 mol%), 0.992 (TL-1 mol%), and 0.994 (CW-OSL-undoped). As mentioned above, the $Sr_2P_2O_7$ and $Sr_2P_2O_7$:Eu^{3+} (0.5 mol%) samples exhibited the most intense CW-OSL and TL response, respectively. The minimum detectable dose (MDD) of the undoped and Eu^{3+} (0.5 and 1 mol%) doped $Sr_2P_2O_7$ samples was calculated using three times the standard deviation (3σ) of three non-irradiated readings (TL and CW-OSL backgrounds) [36]. The MDD values were estimated as 2 mGy (TL-0.5 mol%), 3 mGy (TL-1 mol%), 14 mGy (TL-undoped) and 2 mGy (CW-OSL-undoped). It means that $Sr_2P_2O_7$ and $Sr_2P_2O_7$:Eu^{3+} (0.5 mol%) can be respectively used to detect low doses of ^{90}Sr beta particle radiation using CW-OSL and TL response.

A desirable characteristic in a TL and CW-OSL luminescent material is that it has repeatability, with a standard deviation lower than 5%, after a given number of irradiation and measurements. Therefore, the TL (undoped and Eu^{3+} doped $Sr_2P_2O_7$ with 0.5 and 1 mol %) and CW-OSL (undoped $Sr_2P_2O_7$) repeatability were studied. The samples were irradiated, using ^{90}Sr beta particles at 8 Gy, and measured for ten cycles. The samples showed an acceptable TL and CW-OSL repeatability (Fig. 6) with a variation coefficient (VC) equal to 3.10% (TL-undoped), 0.90% (TL-0.5 mol%), 0.16% (TL-1 mol %) and 0.91% (CW-OSL-undoped).

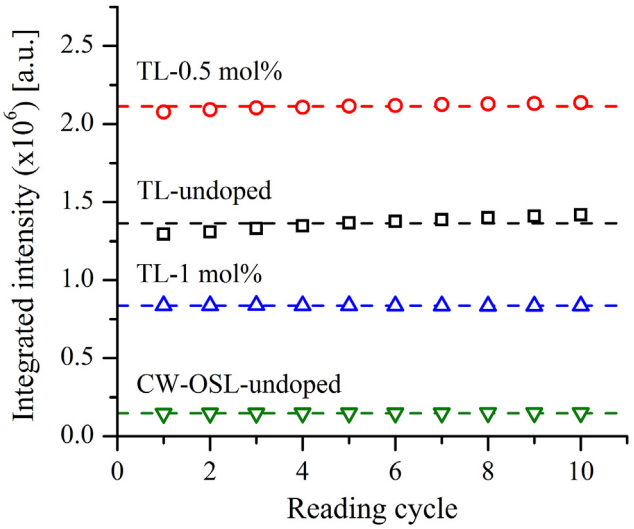

Fig. 6. TL repeatability of $Sr_2P_2O_7$ undoped (black squares) and doped with 0.5 (red circles) and 1 mol% (blue triangles) Eu^{3+}, and CW-OSL repeatability of undoped $Sr_2P_2O_7$ (green triangles). Dashed lines represent the mean of the measurements. (For interpretation of the references to colour in this figure legend, the reader is referred to the Web version of this article.)

TL and CW-OSL fading response (UV-blue region) were investigated in undoped and Eu^{3+} (0.5 and 1 mol%) doped $Sr_2P_2O_7$ samples, they were irradiated to 8 Gy of ^{90}Sr beta particles, stored at room temperature in the dark and analyzed (TL and CW-OSL) after different intervals of time (0.5, 1, 3, 6, 18, 24 72 and 120 h). After each CW-OSL response the sample was cleaned with a TL readout from RT to 300 °C and 2 °C/s heating rate. The first value (reference) was measured immediately after irradiation. In Fig. 7 is shown the results of the fading study. In the first 24 h the intensity of the samples strongly decayed due to the thermal instability of the shallow traps which are related to the maxima at low temperature

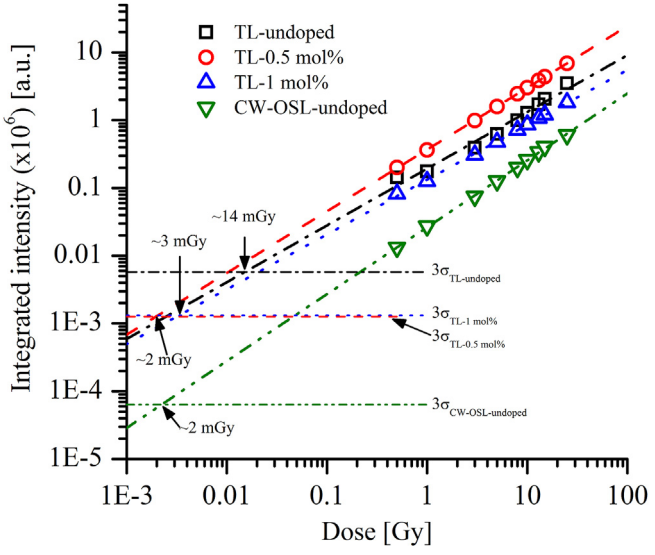

Fig. 5. TL dose response of $Sr_2P_2O_7$ (black squares) and $Sr_2P_2O_7$:Eu^{3+} doped at 0.5 (red circles) and 1 mol% (blue triangles), and CW-OSL dose response of $Sr_2P_2O_7$ (green triangles). Both TL and CW-OSL response was analyzed in the dose range 0.5–25 Gy. Horizontal lines represent the 3σ value of three TL and CW-OSL background measurements. (For interpretation of the references to colour in this figure legend, the reader is referred to the Web version of this article.)

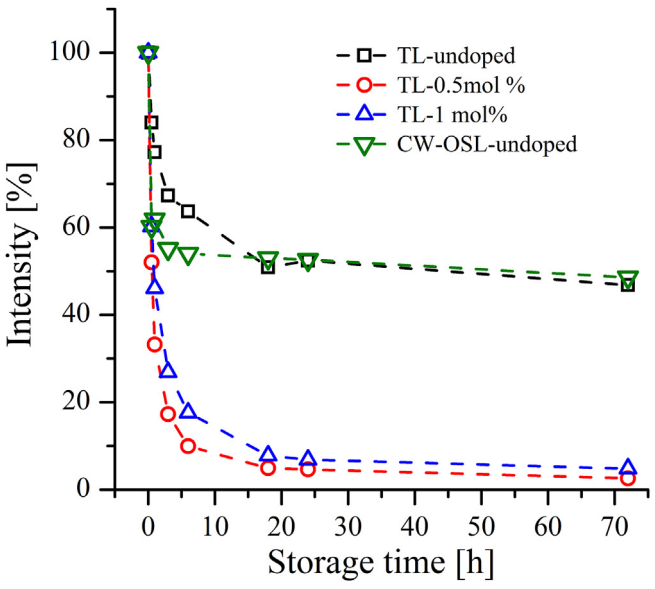

Fig. 7. Fading of undoped (TL and CW-OSL) and Eu^{3+} (TL-0.5 and 1 mol%) doped $Sr_2P_2O_7$ monitoring up to 72 h after irradiation. The samples were irradiated to 8 Gy and storage in dark at RT.

in the undoped (95 °C) and Eu^{3+} doped (79 and 85 °C) materials. The undoped sample shows the less TL and CW-OSL fading after 72 h of stored with amount around 50% compared with the reference. Before 24 h the CW-OSL response displayed a fading rate faster than the TL response and at 18 h the TL and CW-OSL fading shows similar decayed. This behavior is due to that the first TL maximum (95 °C) contributes more in the formation of the CW-OSL decay curve than the second maximum (150 °C) which is thermally stable after 24 h of storage. Eu^{3+} (0.5 and 1 mol%) doped samples showed similar trends with TL intensity decay around 95% after 72 h because the maximum at low temperature (79 and 85 °C) exhibits strong fading during the storage in the dark at RT.

4. Conclusions

The solvent evaporation method was successful to synthesize undoped and Eu^{3+} (0.5, 1, 3, 5, 8 and 10 mol%.) doped $Sr_2P_2O_7$ phosphors. Photoluminescence excitation and emission spectra showed characteristics 4f→5d transitions associated with the presence of Eu^{3+} ions into the $Sr_2P_2O_7$ host lattice. The PL excitation spectrum displayed an intense charge transfer band centered at 267 nm which is related to the charge transference between Eu^{3+} and O^{2-} ions. PL concentration quenching appears in the phosphors doped with Eu^{3+} concentrations higher than 5 mol%. The thermoluminescence response of the $Sr_2P_2O_7$:Eu^{3+} samples measured using a set of filters at 414 nm (UV-blue region) and 575 nm (green-yellow region) confirms that the ^{90}Sr beta particles cause a chemical reduction process in the Eu^{3+} ions which change the valence state to Eu^{2+} ions. Thermoluminescence response of the $Sr_2P_2O_7$:Eu^{3+} material analyzed in the UV-blue region displays the formation of at least two peaks around 79–90 and 148–162 °C associated with the Eu^{2+} blue emissions. The TL glow curve of undoped $Sr_2P_2O_7$ is composed by three peaks at 95, 150 and 230 °C. CW-OSL response of undoped and doped $Sr_2P_2O_7$:Eu^{3+} (0.5 and 1 mol%) was studied for the first time. All $Sr_2P_2O_7$ and $Sr_2P_2O_7$:Eu^{3+} (0.5 and 1 mol%) samples exhibited a linear TL and CW-OSL dose response from 0.5 to 25 Gy and acceptable repeatability after ten cycles of irradiation and reading. A minimum ^{90}Sr beta particle dose of 2 mGy can be detected by $Sr_2P_2O_7$ and $Sr_2P_2O_7$:Eu^{3+} (0.5 mol%) samples using CW-OSL and TL dose-response. The TL and CW-OSL fading of the undoped sample shows a decay of 50% within the 72 h. In Eu^{3+} doped samples (0.5 and 1 mol%) the fading decayed ~95% after 72 h of storage due to the thermal instability of the low temperature maximum. $Sr_2P_2O_7$ and $Sr_2P_2O_7$:Eu^{3+} (0.5 mol%) samples show interesting PL, TL and CW-OSL emissions. More physical studies are necessary to understand the luminescence processes involved in the CW-OSL and TL response of the undoped and Eu^{3+} doped $Sr_2P_2O_7$ materials.

Acknowledgments

This work was supported by the projects CONACYT-253777 and SIP-IPN-20170883. The author: M. Valverde thanks to CONACYT (México) for her scholarship position. The authors are grateful to Adriana Tejeda (IIM-UNAM) for her help in the X-Ray diffraction measurements.

References

[1] S. Ye, F. Xiao, Y.X. Pan, Y.Y. Ma, Q.Y. Zhang, Phosphors in phosphor-converted white light-emitting diodes: recent advances in materials, techniques and properties, Mater. Sci. Eng. R Rep. 71 (2010) 1–34.
[2] N.P. Patel, M. Srinivas, V. Verma, D. Modi, K.V.R. Murthy, Investigation of dosimetric features of beta - irradiated Er^{3+} doped strontium pyrophosphate, Adv. Mater. Lett. 7 (2016) 497–500.
[3] S. Ye, Z.S. Liu, J.G. Wang, X.P. Jing, Luminescent properties of $Sr_2P_2O_7$:Eu,Mn phosphor under near UV excitation, Mater. Res. Bull. 43 (2008) 1057–1065.
[4] F. Le, L. Wang, W. Jia, D. Jia, S. Bao, Synthesis and photoluminescence of Eu^{2+} by co-doping Eu^{3+} and Cl^- in $Sr_2P_2O_7$ under air atmosphere, J. Alloys. Compd. 512 (2012) 323–327.
[5] R.C. Ropp, Luminescence and the Solid State, second ed., Elsevier, Amsterdam, 2004.
[6] R. Pang, C. Li, L. Shi, Q. Su, A novel blue-emitting long-lasting pyrophosphate phosphor $Sr_2P_2O_7$:Eu^{2+},Y^{3+}, J. Phys. Chem. Solid. 70 (2009) 303–306.
[7] M. Peng, L. Wondraczek, Photoluminescence of $Sr_2P_2O_7$:Bi^{2+} as a red phosphor for additive light generation, Opt. Lett. 35 (2010) 2544–2546.
[8] G.D. Fan, C. Lin, D. Fan, B.J. Liu, W. Yang, Improved luminescent properties of Eu^{3+} activated phosphor α-$Sr_2P_2O_7$ by charge compensation, J. Mater. Sci. Electron. 27 (2016) 892–898.
[9] V. Natarajan, M.K. Bhide, A.R. Dhobale, S.V. Godbole, T.K. Seshagiri, A.G. Page, C.H. Lu, Photoluminescence, thermally stimulated luminescence and electron paramagnetic resonance of europium-ion doped strontium pyrophosphate, Mater. Res. Bull. 39 (2004) 2065–2075.
[10] N.P. Patel, M. Srinivas, D. Modi, V. Vishwnath, K.V.R. Murthy, Luminescence study and dosimetry approach of Ce on an α-$Sr_2P_2O_7$ phosphor synthesized by a high-temperature combustion method, Luminescence 30 (2015) 472–478.
[11] N.P. Patel, M. Srinivas, D. Modi, V. Verma, K.V.R. Murthy, Optimization of luminescence properties of Tb^{3+}-doped α-$Sr_2P_2O_7$ phosphor synthesized by combustion method, Rare Met. (2016) 1–7.
[12] T. Zhou, X. Jiang, C. Zhong, X. Tang, S. Ren, Y. Zhao, M. Liu, X. Lai, J. Bi, D. Gao, Hydrothermal synthesis of controllable size, morphology and optical properties of β-$NaGdF_4$:Eu^{3+} microcrystals, J. Lumin. 175 (2016) 1–8.
[13] L. Wang, M. Xu, R. Sheng, L. Liu, D. Jia, Microwave assisted co-precipitation synthesis and photoluminescence characterization of spherical $Sr_2P_2O_7$:Ce^{3+}, Tb^{3+} phosphors, J. Alloys. Compd. 579 (2013) 343–347.
[14] M.J. Xu, L.X. Wang, D.Z. Jia, L. Liu, L. Zhang, Z.P. Guo, R. Sheng, Morphology tunable self-assembled $Sr_2P_2O_7$:Ce^{3+}, Mn^{2+} phosphor and luminescence properties, J. Am. Ceram. Soc. 96 (2013) 1198–1202.
[15] L. Mariscal, S. Carmona-Téllez, G. Alarcón-Flores, H. Murrieta, J.M. Hernández, E. Camarillo, C. Falcony, Luminescent properties of Al_2O_3:Tb^{3+} powders embedded in polyethylene terephthalate films, Opt. Mater. 46 (2015) 233–239.
[16] L. Mariscal-Becerra, R. Vázquez-Arreguín, U. Balderas, S. Carmona-Téllez, H. Murrieta Sánchez, C. Falcony, Luminescent characteristics of layered yttrium oxide nano-phosphors doped with europium, J. Appl. Phys. 121 (2017), 125111.
[17] J.V. Soares, C.F. Gugliotti, Y.S. Kawashima, S.H. Tatumi, J.C.R. Mittani, Thermoluminescence and optically stimulated luminescence characteristics of Al_2O_3 doped with Tb, Radiat. Meas. 71 (2014) 78–80.
[18] Y.S. Kawashima, C.F. Gugliotti, M. Yee, S.H. Tatumi, J.C.R. Mittani, Thermoluminescence features of MgB_4O_7:Tb phosphor, Radiat. Phys. Chem. 95 (2014) 91–93.
[19] R.S. Palaspagar, R.P. Sonekar, S.K. Omanwar, NUV excited luminescence of Eu^{3+} doped inorganic $NaCa_{0.5}Al_2B_2O_7$ phosphor via slow evaporation technique, J. Mater. Sci. Mater. Electron. 27 (2016) 9335–9340.
[20] P. Du, J.S. Yu, Photoluminescence and cathodoluminescence properties of Eu^{3+} ions activated $AMoO_4$ (A=Mg, Ca, Sr, Ba) phosphors, Mater. Res. Bull. 70 (2015) 553–558.
[21] J. Wang, Y. Cheng, Y. Huang, P. Cai, S. Il Kim, H.J. Seo, Structural and luminescent properties of red-emitting Eu^{3+} -doped ternary rare earth antimonates R_3SbO_7 (R = La, Gd, Y), J. Mater. Chem. C 2 (2014) 5559–5569.
[22] S.H. Lee, P. Du, L.K. Bharat, J.S. Yu, Ultraviolet radiation excited strong red-emitting $LaAlO_3$:Eu^{3+} nanophosphors: synthesis and luminescent properties, Ceram. Int. 43 (2017) 4599–4605.
[23] C. Boronat, T. Rivera, J. Garcia-Guinea, V. Correcher, Cathodoluminescence emission of REE (Dy, Pr and Eu) doped $LaAlO_3$ phosphors, Radiat. Phys. Chem. 130 (2017) 236–242.
[24] T. Kano, Principal phosphor materials and their optical properties, in: W.M. Yen, S. Shionoya, H. Yamamoto (Eds.), Fundamental of Phosphors, CRC Press, Boca Raton, London, New York, 2006, pp. 181–204.
[25] X. Zhang, C. Zhou, J. Song, L. Zhou, M. Gong, High-brightness and thermal stable $Sr_3La(PO_4)_3$:Eu^{3+} red phosphor for NUV light-emitting diodes, J. Alloys. Compd. 592 (2014) 283–287.
[26] R.J. Amjad, W. Santos, C. Jacinto, M.R. Dousti, Luminescence dynamics in Eu^{3+} doped fluoroborate glasses, J. Lumin. 192 (2017) 827–831.
[27] B. Han, P. Li, J. Zhang, J. Zhang, Y. Xue, H. Shi, The effect of Li^+ ions on the luminescent properties of a single-phase white light-emitting phosphor α-$Sr_2P_2O_7$:Dy^{3+}, Dalton Trans. 44 (2015) 7854–7861.
[28] S.V. Upadeo, S.V. Moharil, Redox reactions and thermoluminescence in some europium-doped phosphates, J. Phys. Condens. Matter 7 (1995) 957–963.
[29] S. Seyyidoğlu, M. Özenbaş, N. Yazıcı, A. Yılmaz, Investigation of solid solution of ZrP_2O_7–$Sr_2P_2O_7$, J. Mater. Sci. 42 (2007) 6453–6463.
[30] V. Dubey, J. Kaur, S. Agrawal, Effect of europium concentration on photoluminescence and thermoluminescence behavior of Y_2O_3:Eu^{3+} phosphor, Res. Chem. Intermed. 41 (2015) 4727–4739.
[31] Y. Parganiha, J. Kaur, V. Dubey, D. Chandrakar, Synthesis, characterization, thermoluminescence and optical studies of Eu^{3+} doped Y_2SiO_5 phosphor, Superlattice. Microst. 77 (2015) 152–161.
[32] J. Kaur, Y. Parganiha, V. Dubey, D. Singh, D. Chandrakar, Synthesis, characterization and luminescence behavior of ZrO_2:Eu^{3+},Dy^{3+} with variable concentration of Eu and Dy doped phosphor, Superlattice. Microst. 73 (2014)

38–53.
[33] A.N. Yazici, S. Seyyidolu, H. Toktamiş, A. Yilmaz, Thermoluminescent properties of $Sr_2P_2O_7$ doped with copper and some rare earth elements, J. Lumin. 130 (2010) 1744–1749.
[34] A. Barrera-Villatoro, C. Boronat, T. Rivera-Montalvo, V. Correcher, J. Garcia-Guinea, J. Zarate-Medina, Cathodo- and thermally stimulated luminescence characterization of synthetic calcium phosphates, Spectrosc. Lett. 51 (2018) 22–26.
[35] N.P. Patel, V. Verma, D. Modi, K.V.R. Murhty, M. Srinivas, Thermoluminescence kinetic features of Eu^{3+} doped strontium pyrophosphate after beta irradiation, RSC Adv. 6 (2016) 77622–77628.
[36] J.V. Soares, C.F. Gugliotti, Y.S. Kawashima, S.H. Tatumi, J.C.R. Mittani, Thermoluminescence and optically stimulated luminescence characteristics of Al_2O_3 doped with Tb, Radiat. Meas. 71 (2014) 78–80.